Centralized voltage control for distribution networks with embedded PV systems

(Article begins on next page)

28 November 2024

# Centralized voltage control for distribution networks with embedded PV systems

A. Cagnano[*], E. De Tuglie

*Dipartimento di Ingegneria Elettrica e dell'Informazione — DEI, Politecnico di Bari, Via Re David, 200, 70125 Bari, Italy*

## A B S T R A C T

This paper proposes a centralized control methodology for optimizing nodal voltages of distribution networks by acting on the reactive power produced by PV-inverters. Control actions are centrally evaluated in real-time by solving a constrained dynamic optimization problem aimed at minimizing the voltage deviation from a reference value. The solution of this problem is obtained by adopting an algorithm operating in the continuous time domain based on a fast artificial dynamic system involving the sensitivity theory. By this approach the controller is able to promptly respond to any change in the system operating point, allowing its adoption in the continuous time domain. However, it must be considered that the injection of the reactive power provided by PV-inverters entails greater conduction and switching losses, causing a reduction in the active power output, thus implying less incomings. As a consequence, these additional operating costs have been analyzed and evaluated in order to establish an economic compensation mechanism able to guarantee fair reimbursement to PV generators engaged in this regulation service. Computer simulations performed on an MV distribution system, demonstrate the effectiveness of the proposed control scheme under different operating conditions, confirming its ability to control the network in real-time.

## 1. Introduction

The intensive economic support programs adopted by the Italian Government [1] in recent years have resulted in a proliferation of Distributed Generators (DGs) and, more specifically, of Photovoltaic (PV) plants. The high degree of penetration of such sources requires a complete revision of existing practices of distribution systems operation. In fact, these generators, depending on their specific characteristics and location, significantly affect the voltage profile, network losses and fault levels [2—6]. All these factors can limit the full exploitation of such resources if adequate control actions and ancillary service providers are not available in the grid. Among possible providers, PV plants seem to be particularly attractive because of their power electronic converters even if, until now, this possibility has not been fully exploited due to the lack of adequate control methodologies. For this reason, some interconnection standards [7,8] imposing a unitary power factor at connection points have excluded these plants from the regulation service. More recently, thanks to scientific and technology improvements, this opportunity seems to be practicable. Therefore, new grid codes developed in many countries [9—17] require that new PV inverters must incorporate any reactive control signals coming from the network operator. However, the issue on how to control such devices in real time is still pending even if a lot of research is being carried out on this topic and, particularly, on the voltage regulation problem aimed at satisfying the standard EN 50160 [18]. Technical literature extensively reports methods based on Genetic Algorithm (GA), Particle Swarm Optimization (PSO), Evolutionary PSO (EPSO), Discrete PSO (DPSO) and sensitivity theory [19—30]. In these works, control actions are centrally evaluated by solving a constrained optimization problem to minimize system losses. Control variables are the reactive powers supplied by PV-inverters, transformer taps and all other voltage control devices. Nodal voltages constitute the set of inequality constraints, thus disregarding the optimum condition on voltage levels. With these methodologies, the optimum condition is usually achieved by increasing the voltage profile, and then reducing current flows, until voltages at some nodes reach their limits. In this case, unpredicted events (sudden overloads, excursion of solar radiations or wind gusts), may bring voltages over the specified limits

---

* Corresponding author. Tel.: +39 080 5963422; fax: +39 080 5963410.
  *E-mail address:* alessia.cagnano@poliba.it (A. Cagnano).

resulting in the nuisance of voltage relays tripping and cascade events. For this reason, it is advisable to directly focus on the optimization of the voltage profile, as we propose in this paper. In doing this, voltage deviations from a reference value are minimized by managing the reactive power provided by PV inverters by solving a constrained dynamic optimization problem. The methodology involves a fictitious dynamic system based on the Lyapunov function that guarantees the existence of a solution.

Additionally, it must be considered that the supplementary injection of reactive power increases inverter losses, thus minimizing PV incomes. In order to stimulate the provision of this important ancillary service, this loss of profits should require an economic compensation mechanism able to guarantee a fair reimbursement to PV generators engaged in this regulation service. With this aim a section of this paper is devoted to analyzing this economic impact.

Several computer simulations have been performed on a typical MV distribution network in order to test performance of the controller developed. The results obtained demonstrate that the controller is able to promptly respond to any change in the system operating point, confirming its ability to control the voltage profile in real-time. Moreover, as an additional output, the algorithm allows the *a-posteriori* costs corresponding to each control action to be evaluated on the basis of the feed in tariff plus the market clearing price for the energy not supplied due to additional inverter losses.

## 2. Reactive power control method

From a mathematical point of view, the voltage control problem can be stated as an optimization problem aimed at minimizing the voltage deviation from a reference value.

The basic elements of the optimization procedure are defined as follows.

### 2.1. The objective function

Denoting the vector of nodal voltage magnitude measurements with $\boldsymbol{V}(\boldsymbol{Q}_{PV})$ and the vector of nodal reference voltage magnitudes at all buses with $\boldsymbol{V}_{ref}$, the vector of the control error can be defined as follows:

$$\boldsymbol{e}_V = \boldsymbol{V}(\boldsymbol{Q}_{PV}) - \boldsymbol{V}_{ref} \tag{1}$$

where $\boldsymbol{Q}_{PV}$ represents the vector of control variables, i.e. reactive powers injected by photovoltaic plants. The aim is to regulate $\boldsymbol{Q}_{PV}$ until $\boldsymbol{e}_V$ is either zero or minimal. For this purpose, the following performance index, $V$, is assumed:

$$V(\boldsymbol{e}_V) = \frac{1}{2}\boldsymbol{e}_V^T \boldsymbol{W} \boldsymbol{e}_V \tag{2}$$

where $\boldsymbol{W}$ is a symmetric positive definite matrix whose coefficients weight individual components of the performance index. Note that we have defined this function according to the methodology developed in Ref. [29] to be a Lyapunov function that guarantees the existence of a mathematical solution.

The optimization of the performance index (2) requires the following equality and inequality constraints to be satisfied.

### 2.2. Equality constraints

$$\boldsymbol{f}(\boldsymbol{x}, \boldsymbol{u}, \boldsymbol{Q}_{PV}) = 0 \tag{3}$$

Eqn. (3) represents the power flow equations, where the state vector $\boldsymbol{x}$ is the nodal voltage vector expressed in terms of
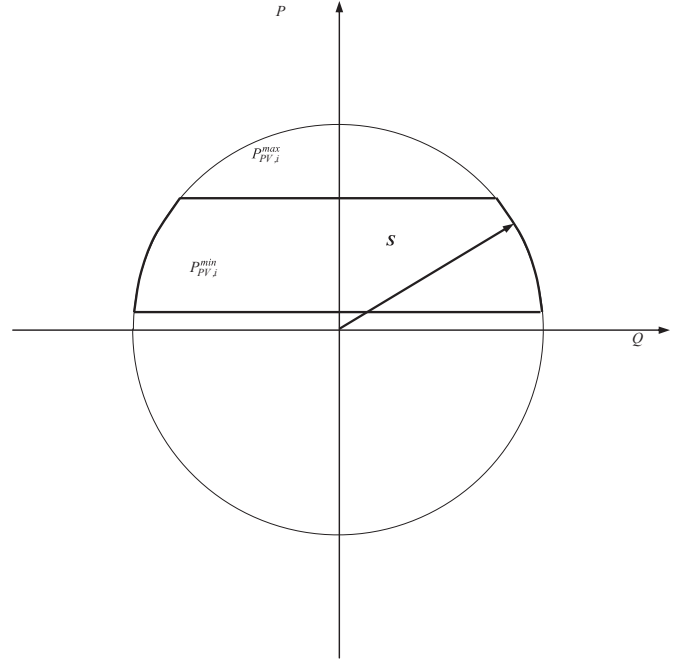


**Fig. 1.** Loading capability chart of the i-th photovoltaic generator.

magnitude and phase $\boldsymbol{x} = [\boldsymbol{V} \quad \vartheta]^T$, and $\boldsymbol{u} = [\boldsymbol{P}_{PV} \quad \boldsymbol{P}_L \quad \boldsymbol{Q}_L]^T$ is a vector whose elements are the active powers injected by all PV generators and active and reactive powers measured at all load buses.

### 2.3. Inequality constraints

To avoid impacting economic benefits deriving from the active power production of photovoltaic plants, the reactive power output must be controlled within the photovoltaic generator's capabilities.

There are mainly two factors influencing the capability of the generic *i-th* PV generator. The first one is the minimum ($P_{PV,i}^{\min}$) and maximum ($P_{PV,i}^{\max}$) injectable active power. $P_{PV,i}^{\min}$ represents the minimum value of production below which the inverter shuts down. $P_{PV,i}^{\max}$ is the nominal power of the DC generator corrected by the efficiency of the overall Balance Of System (BOS), typically equal to 75%.
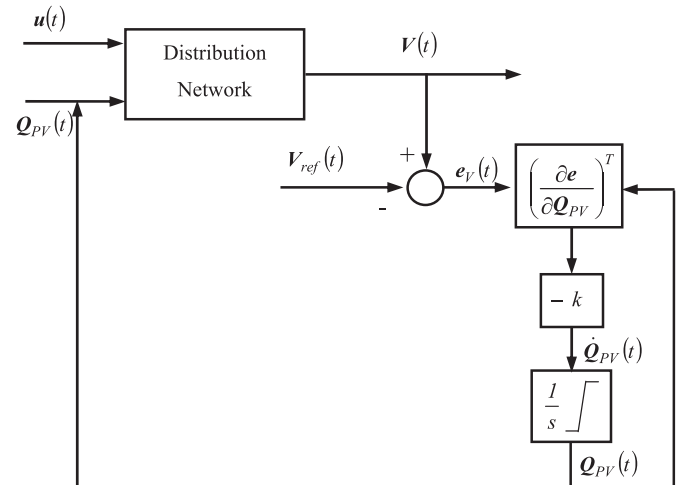


**Fig. 2.** Basic scheme of the proposed methodology.

The second factor limits the maximum current, $I_i^{\max}$, of the $i$-th PV inverter for a constant voltage at the AC side of the inverter. The maximum apparent power capability is described in the $P$–$Q$ plane by a circle centered in the origin having the following radius:

$$S_i^{\max}(V_{ac,i}) = V_{ac,i} \cdot I_i^{\max} \tag{4}$$

In Fig. 1 the derived capability curve of the $i$-th photovoltaic plant is shown.

From a mathematical point of view, the capability curves of all PV generators can be expressed as follows:

$$\begin{cases} \boldsymbol{P}_{PV}^{\min} \le \boldsymbol{P}_{PV} \le \boldsymbol{P}_{PV}^{\max} \\ -\sqrt{\boldsymbol{S}_{\max}^2 - \boldsymbol{P}_{PV}^2} \le \boldsymbol{Q}_{PV} \le \sqrt{\boldsymbol{S}_{\max}^2 - \boldsymbol{P}_{PV}^2} \end{cases} \tag{5}$$

During the optimization process, nodal voltages can experience reach unacceptable levels thus we consider another inequality constraint in order to explicitly force voltage magnitudes to be in the following range:

$$\boldsymbol{V}^{\min} \le \boldsymbol{V} \le \boldsymbol{V}^{\max} \tag{6}$$

### 2.4. The static voltage optimization problem

Under the previously illustrated assumptions, the overall optimization problem can be stated as follows:

$$\min_{\boldsymbol{Q}_{PV}} V(\boldsymbol{e}_V(\boldsymbol{Q}_{PV})) = \min_{\boldsymbol{Q}_{PV}} \frac{1}{2} [\boldsymbol{e}_V(\boldsymbol{Q}_{PV})]^T \boldsymbol{W} \boldsymbol{e}_V(\boldsymbol{Q}_{PV}) \tag{7}$$

subject to

$$\boldsymbol{f}(\boldsymbol{x}, \boldsymbol{u}, \boldsymbol{Q}_{PV}) = 0 \tag{8}$$

$$-\sqrt{\boldsymbol{S}_{\max}^2 - \boldsymbol{P}_{PV}^2} \le \boldsymbol{Q}_{PV} \le \sqrt{\boldsymbol{S}_{\max}^2 - \boldsymbol{P}_{PV}^2}$$

$$\boldsymbol{V}^{\min} \le \boldsymbol{V} \le \boldsymbol{V}^{\max} \tag{9}$$

### 2.5. The dynamic voltage optimization problem

The problem stated in (7) is specified for any fixed operating point. It can be solved by adopting classical solution methods that must be initialized every time an event occurs in the system (event-based trigger mechanism) or at fixed time intervals (time-based
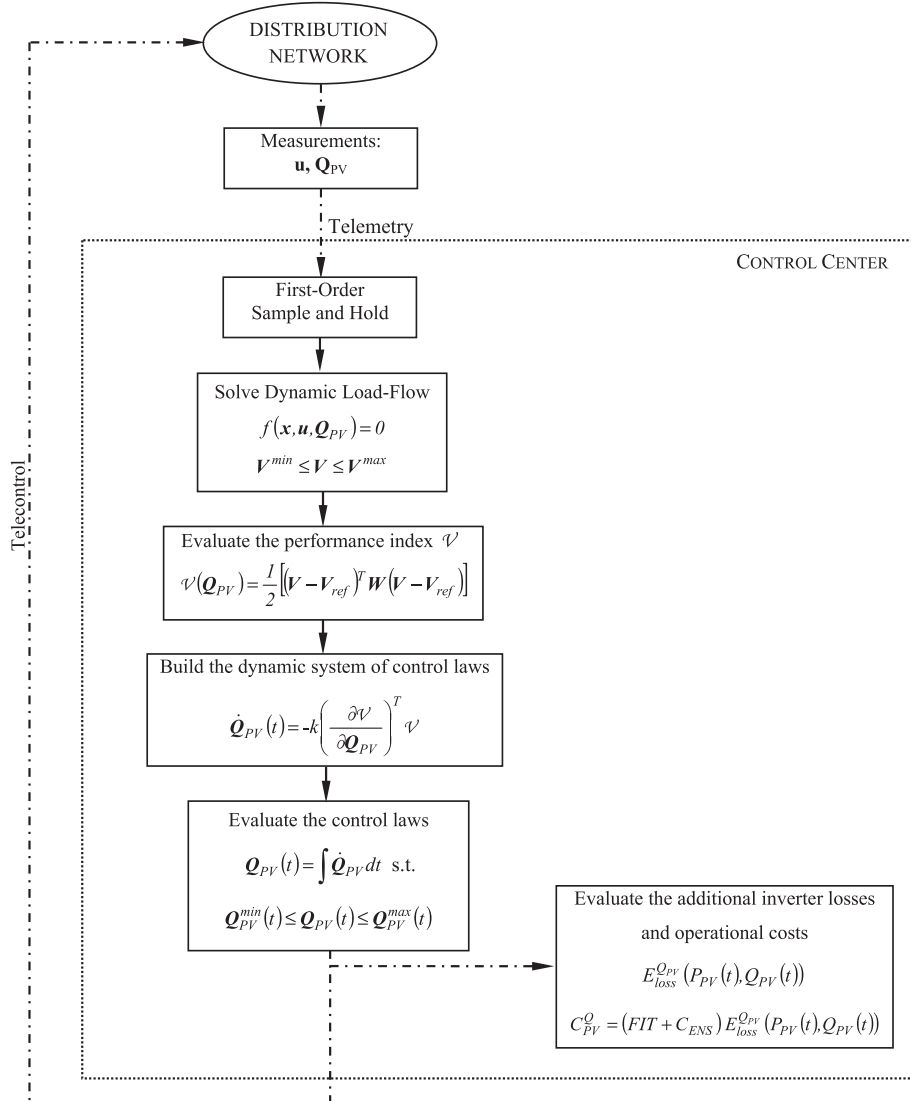


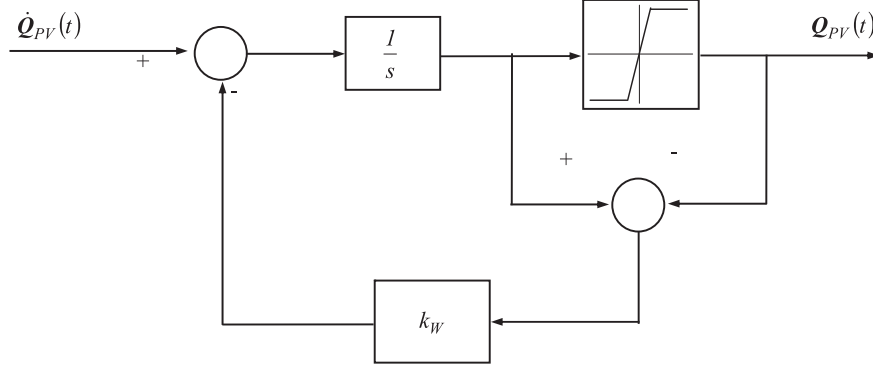**Fig. 3.** Flow-chart of the proposed algorithm.

**Fig. 4.** Basic scheme of the proposed anti-wind-up compensator.

trigger mechanism). If an event-based trigger is adopted, the control scheme would require an event identification system. If a time-based trigger is considered, the time interval must be carefully chosen. If it is too long, some events cannot be captured and processed by the controller, whereas, if it is too short the computational burden could be excessive. In order to overcome these problems, we propose an optimization algorithm operating in the continuous time domain adopting the methodology developed in Ref. [29]. The developed code, fed by data coming into the control center, runs continuously without requiring to be restarted. As a result output signals are changed according to the latest updated information.

The developed methodology is based on the sensitivity theory involving the Lyapunov function and consists of setting up a fictitious dynamic system, whose state variables are represented by control variables $\mathbf{Q}_{PV}$. With this assumption, the solution of the optimization problem can be obtained by finding the equilibrium point (if any) of such a dynamic system. The adoption of the Lyapunov method ensures that an equilibrium point will be reached and this will constitute the minimum of the objective function (7). In this sense the voltage error approaches the origin (or the minimum) asymptotically. When the dynamic system lies at its equilibrium point, if the operating condition changes a different value of $V$ is produced, thus driving the methodology to produce a new set of control variables where $V$ is again at a minimum.

The basic idea of the proposed methodology is shown in Fig. 2.

Note that the controller, fed by voltage measurements on the network, firstly evaluates the voltage control error in the current state of the system. Subsequently, the artificial dynamic system $\dot{\mathbf{Q}}_{PV}(t)$ is derived and then integrated in the time domain in order to obtain control laws as follows:

$$\mathbf{Q}_{PV}(t) = -k \int \left( \frac{\partial \mathbf{e}_V}{\partial \mathbf{Q}_{PV}} \right)^T \mathbf{W}^T \mathbf{e}_V \, \mathrm{d}t \tag{10}$$

In particular, this model contains sensitivities of the voltage error with regard to the control action, $\partial \mathbf{e}_V / \partial \mathbf{Q}_{PV}$. The evaluation of such sensitivities can be obtained as follows:

$$\left( \frac{\partial \mathbf{e}_V}{\partial \mathbf{Q}_{PV}} \right) = \left( \frac{\partial \mathbf{e}_V}{\partial \mathbf{x}} \right) \left( \frac{\partial \mathbf{x}}{\partial \mathbf{Q}_{PV}} \right) \tag{11}$$

where $(\partial \mathbf{x} / \partial \mathbf{Q}_{PV})$ can be expressed as follows:

$$\left( \frac{\partial \mathbf{x}}{\partial \mathbf{Q}_{PV}} \right) = \mathbf{J}(\mathbf{x})^{-1} \left( \frac{\partial \mathbf{S}}{\partial \mathbf{Q}_{PV}} \right) \tag{12}$$

Note that, the dependence of control laws on sensitivities establishes a different participation factor for each PV generator. For

this reason, some generators could be forced to provide more or less reactive power and some of them could even reach their upper or lower limits. Note that if inequality constraints are not violated, the steady-state value of the control error will be zero, otherwise it will be minimal.

## 3. Cost analysis of the PV reactive power support

The new Italian grid codes [11] and [17], oblige investors to adopt power converters able to manage the reactive power according to network exigencies. The provision of the reactive power by PVs entails greater conduction and switching losses on their inverters, causing a reduction of the active power available at generator terminals, thus reducing incomes for PV owners. As a consequence, such lost profits must be adequately compensated to guarantee an adequate reactive generation capacity. In fact, the provision of the reactive power could follow one of two ways: a forced commission or voluntary participation in a reactive power market. In the first case, the knowledge of the reactive power production costs can be usefully adopted as the starting point for a
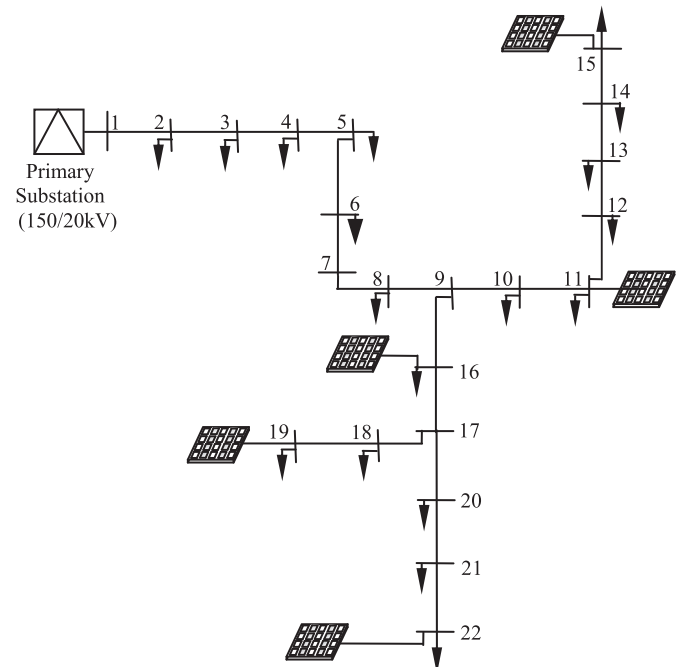


**Fig. 5.** Single-line diagram of the test system.

fair negotiation between the Regulatory Commission and PV owners. In the second case, PV owners will be able to take advantage of this analysis which will give them the possibility to participate in the market with a better knowledge of their costs. In this sense, they could offer this ancillary service with an offer price at least equal to their reactive power production costs. Our analysis, as also suggested in Refs. [31–34], considers that modern converters do not incur additional investment costs for this additional service. For this reason, only operating costs will be examined in this Section.

For a given *i-th* PV inverter the greater conduction and switching losses caused by the provision of the reactive power can be evaluated through the following second order polynomial approximation [32]:

$$
\begin{aligned}
P_{loss,i}(S_i(t)) &= \alpha_i + \beta_i S_i(t) + \gamma_i S_i^2(t) \\
&= \alpha_i + \beta_i\left(\sqrt{P_{PV,i}^2(t) + Q_{PV,i}^2(t)}\right) + \\
&\quad + \gamma_i\left(P_{PV,i}^2(t) + Q_{PV,i}^2(t)\right)
\end{aligned}
\tag{13}
$$

where $S_i$ represents the apparent power of the generic *i-th* inverter and $\alpha_i$, $\beta_i$, and $\gamma_i$ are loss coefficients denoting, respectively, standby losses, voltage dependent losses and current dependent losses. The additional energy losses over time due to the reactive power control, $E_{loss,i}^{Q_{pv}}$, can be evaluated as the difference between the daily energy lost with and without the reactive power control:

$$
\begin{aligned}
E_{loss,i}^{Q_{pv}}(P_{PV,i}(t), Q_{PV,i}(t)) &= \int_{t0}^{t} P_{loss,i}(P_{PV,i}(\tau), Q_{PV,i}(\tau))\, \mathrm{d}\tau \\
&\quad - \int_{t0}^{t} P_{loss,i}(P_{PV,i}(\tau), 0)\, \mathrm{d}\tau
\end{aligned}
\tag{14}
$$

It is assumed that the provision of reactive power is justified if the owners of PV generators get incentives almost equal to those corresponding to the energy not supplied due the increased losses for the reactive power control. We assume that additional energy losses evaluated by means of (14), will be paid at the same price that is paid for the active energy injected into the grid. In this sense, the *i-th* owner of the PV generator must be paid for the reactive power service as follows:

$$
C_{PV,i}^{Q} = (FIT_i + C_{ENS}(t))\, E_{loss,i}^{Q_{pv}}(P_{PV,i}(t), Q_{PV,i}(t))
\tag{15}
$$

where $FIT_i$ is the feed-in-tariff rate assigned to the *i-th* generator, depending on the type and size of the specific PV plant, and $C_{ENS}$ is the market clearing price for the energy not supplied.

## 4. The implementation of the proposed controller

The overall optimization problem can be implemented on the basis of the flow chart shown in Fig. 3.

Measurements on the distribution network are sent to the control center by the classic available telemetry system operating with sampled data. Since our methodology operates in the continuous time domain, we process available data with a first order sample-and-hold block. If one sample is delayed or even missed, the output of this block goes on in feeding the algorithm in the continuous time domain. The derived function is then passed to the Dynamic Load Flow block [35]. This block also incorporates a switching mechanism, from PQ to PV bus types, in order to fix the voltage magnitude at bus experiencing values exceeding the admissible range. The output of the previous block is used to evaluate

**Table 1**
Dynamic Load Flow Report in the non-optimized condition.

| Bus [#] | Voltage | | Generation | | Load | | $e_V^i$ [kV] |
|---|---|---|---|---|---|---|---|
| | Magnitude [kV] | Angle [deg] | Active power [MW] | Reactive power [MVAr] | Active power [MW] | Reactive power [MVAr] | |
| 1 | 20.00 | 0.000 | 9.524 | 4.364 | 0.00 | 0.00 | 0.00 |
| 2 | 19.89 | −0.178 | 0 | 0 | 1.01 | 0.29 | −0.11 |
| 3 | 19.81 | −0.296 | 0 | 0 | 0.80 | 0.23 | −0.19 |
| 4 | 19.72 | −0.407 | 0 | 0 | 1.01 | 0.29 | −0.28 |
| 5 | 19.61 | −0.523 | 0 | 0 | 0.80 | 0.23 | −0.39 |
| 6 | 19.53 | −0.604 | 0 | 0 | 0.30 | 0.09 | −0.47 |
| 7 | 19.45 | −0.681 | 0 | 0 | 0.00 | 0.00 | −0.55 |
| 8 | 19.38 | −0.748 | 0 | 0 | 1.01 | 0.29 | −0.62 |
| 9 | 19.32 | −0.801 | 0 | 0 | 0.00 | 0.00 | −0.68 |
| 10 | 19.26 | −0.807 | 0 | 0 | 1.01 | 0.29 | −0.74 |
| 11 | 19.22 | −0.804 | 2 × 0.5 | 0 | 1.01 | 0.29 | −0.78 |
| 12 | 19.18 | −0.812 | 0 | 0 | 1.01 | 0.29 | −0.82 |
| 13 | 19.15 | −0.813 | 0 | 0 | 1.01 | 0.29 | −0.85 |
| 14 | 19.14 | −0.807 | 0 | 0 | 1.01 | 0.29 | −0.86 |
| 15 | 19.15 | −0.788 | 2 × 0.5 | 0 | 0.50 | 0.15 | −0.85 |
| 16 | 19.31 | −0.794 | 2 × 0.5 | 0 | 1.01 | 0.29 | −0.69 |
| 17 | 19.30 | −0.792 | 0 | 0 | 0.00 | 0.00 | −0.70 |
| 18 | 19.29 | −0.789 | 0 | 0 | 1.01 | 0.29 | −0.71 |
| 19 | 19.28 | −0.769 | 2 × 0.5 | 0 | 1.01 | 0.29 | −0.72 |
| 20 | 19.30 | −0.776 | 0 | 0 | 0.00 | 0.00 | −0.70 |
| 21 | 19.30 | −0.757 | 0 | 0 | 0.50 | 0.15 | −0.70 |
| 22 | 19.31 | −0.735 | 2 × 0.5 | 0 | 0.30 | 0.09 | −0.69 |

the Performance Index of the system in its current state by means of Eqn. (2). Subsequently, the artificial dynamic system is derived and then integrated in the time domain in order to obtain the desired control laws to be processed by local controllers of PV inverters.

Inequality constraints deriving from capability curves of photovoltaic plants are also included in the control loop by adopting thresholds on the integral function. In doing this, in order to avoid saturations giving adverse effects on control performances [36], we suggest using the anti-wind-up compensator shown in Fig. 4.

The gain factor $k$ appearing in the artificial dynamic model $\dot{Q}_{PV}(t)$ significantly influences the overall computational performance. If it is set too large, the procedure rapidly reaches the solution, otherwise the process takes too much time. The suitable
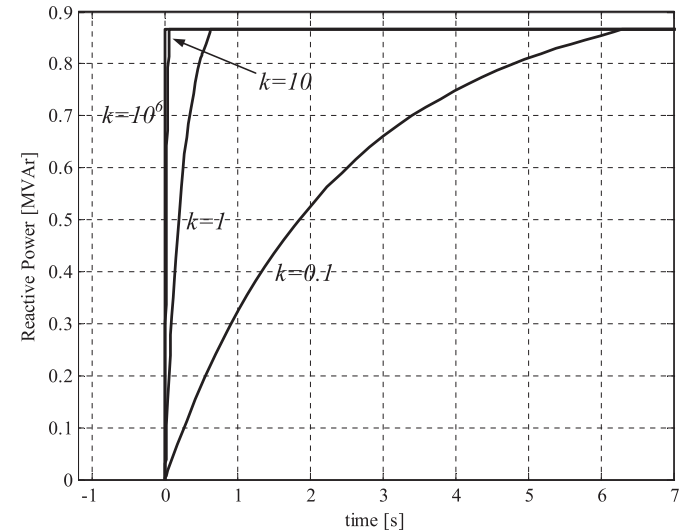


**Fig. 6.** Computational Performances for different values of the gain factor.

choice of this factor cannot be made regardless of the dynamic performance of the grid and this is discussed in the following Section.

## 5. Test results

We tested the proposed methodology on the distribution network shown in Fig. 5 and the data are reported in Appendix A. It consists of a typical MV (20 kV) distribution system with a single transformer substation 150/20 kV located at bus 1, feeding five PV plants, each of them composed by two inverters having the same characteristics. In particular, we assumed the adoption of commercially available

Conergy CSI 1000 inverters [37] giving rise to a maximum allowable apparent power for each PV plant equal to 2 MVA.

All computer simulations were carried out using the software package Matlab/Simulink [38].

In order to demonstrate the effectiveness of the proposed methodology, the three following cases, corresponding to different operating conditions, were investigated:

- **Test 1 − Fixed loads.** This test was performed in order to check the controller's ability to correctly move the system to an optimal point, just providing a 'snapshot' operating condition of the grid.
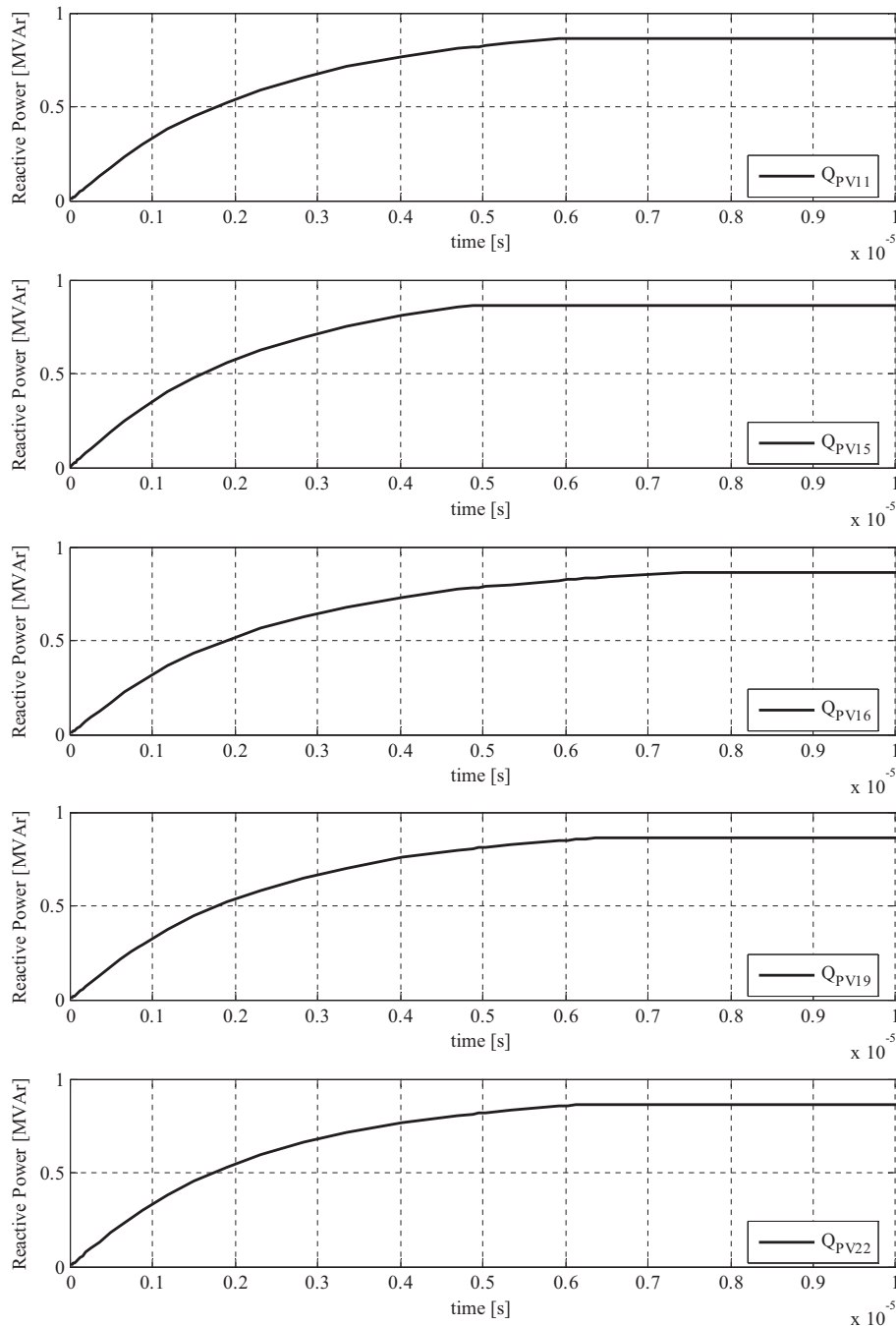


Fig. 7. Reactive power control laws of each of the two inverters of all PV plants.
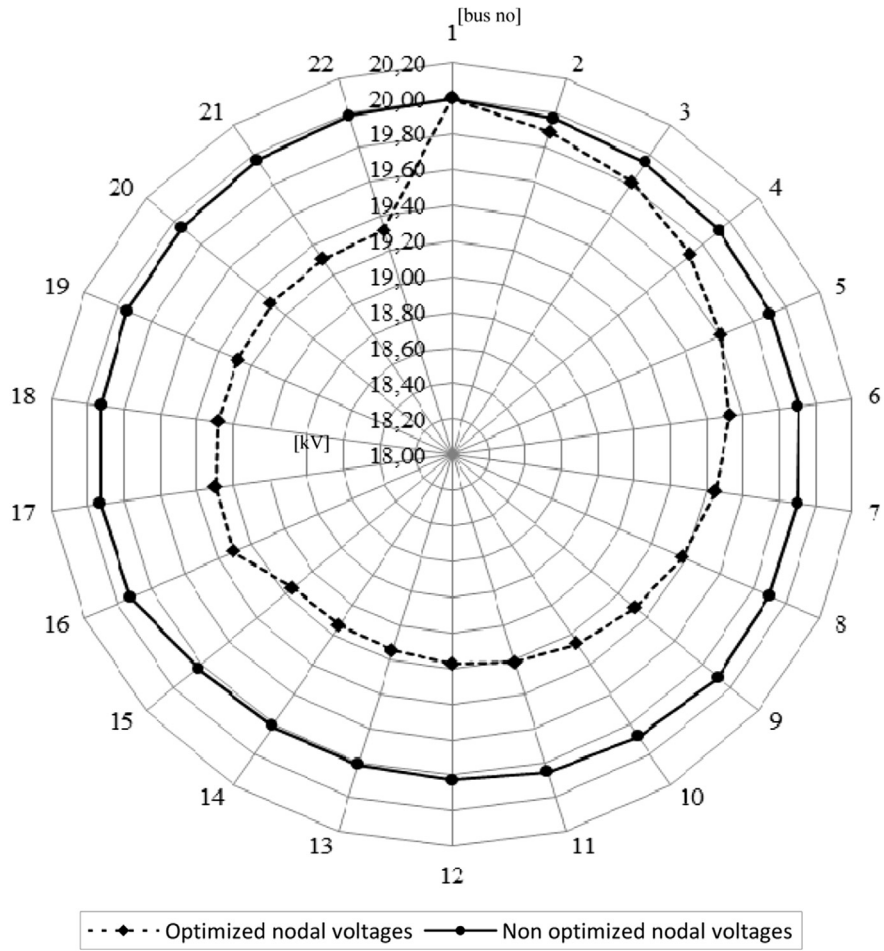
**Fig. 8.** Polar diagram of the nodal voltages with (solid line) and without (dotted line) the reactive power control.
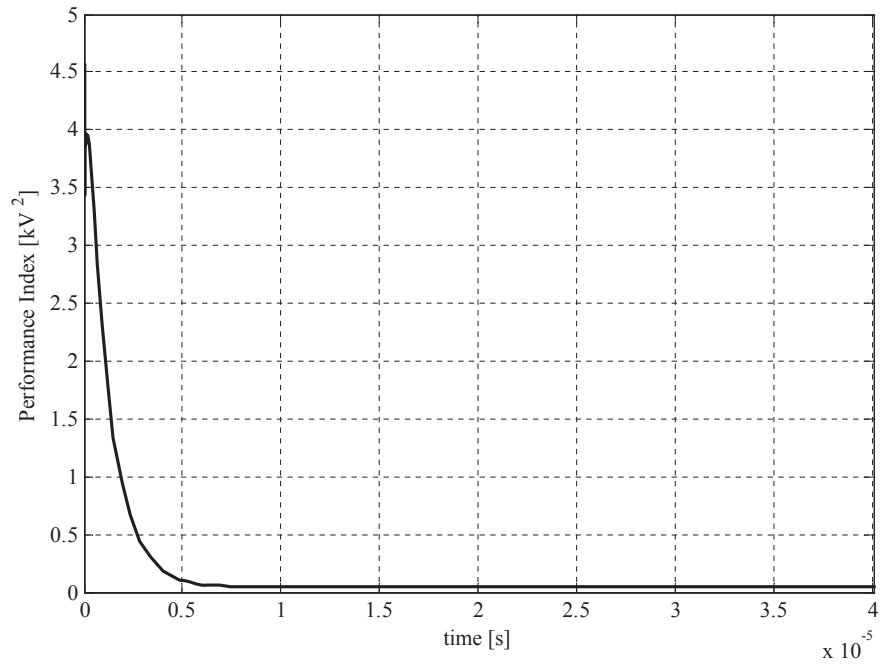


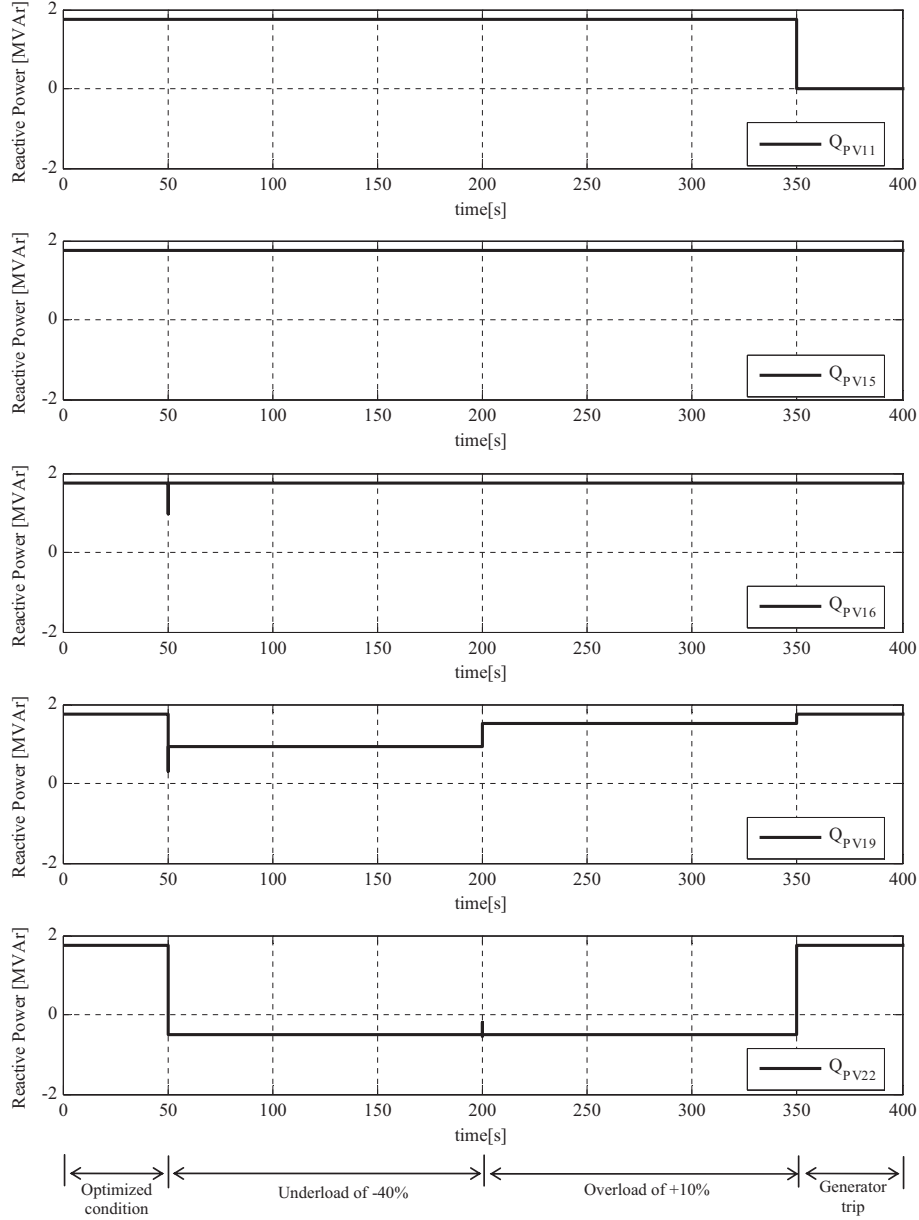**Fig. 9.** Time domain behavior of the Performance Index *V*.

**Fig. 10.** —Reactive power control laws at the PV-inverters.

- **Test 2** − **Sequential events** − **underload, overload and generator trip.** The aim of this test was to analyze dynamic performances of the controller, following sudden burdensome events.
- **Test 3** − **Real-time operation.** This test was conducted to evaluate the controller's aptitude to operate in real time, simulating daily fluctuations of the total load and the total PV generation.

For all tests, we assumed the nominal voltage to be the reference value ($V_{ref} = 20$ kV).

### 5.1. Test 1 − fixed loads

We assumed a snapshot of the system having a pre-defined total load and generation. In particular, we forced each PV plant to inject an active power equal to $2 \times 0.5$ MW. This system condition was

assumed to be the base case. In this case the maximum allowable reactive power that one PV inverter can provide ranges in the interval [-0.866, 0.866]. Starting from this operating point, the dynamic load flow gave rise to the system state reported in Table 1.

For this non optimized condition, in the last column we report the voltage error evaluated for each $i$-th bus ($e_V^i = V_i - V_{ref}$).

To start up the algorithm, an adequate value of the gain factor $k$ has to be chosen. For this reason a preliminary test was performed to investigate the influence of the gain factor $k$ on the transient response of the dynamic system, $\dot{Q}_{PV}$. We performed four optimizations, adopting four different values of $k$ in the range [$10^{-1}$, $10^{6}$]. In Fig. 6 we only report the time domain behavior of the reactive power injected by the two PV-inverters connected at bus #11. As can be noted, with higher values of the gain factor $k$, the dynamic system rapidly reaches its steady-state equilibrium point. We suggest adopting the highest value we used, $k = 10^{6}$, giving rise to
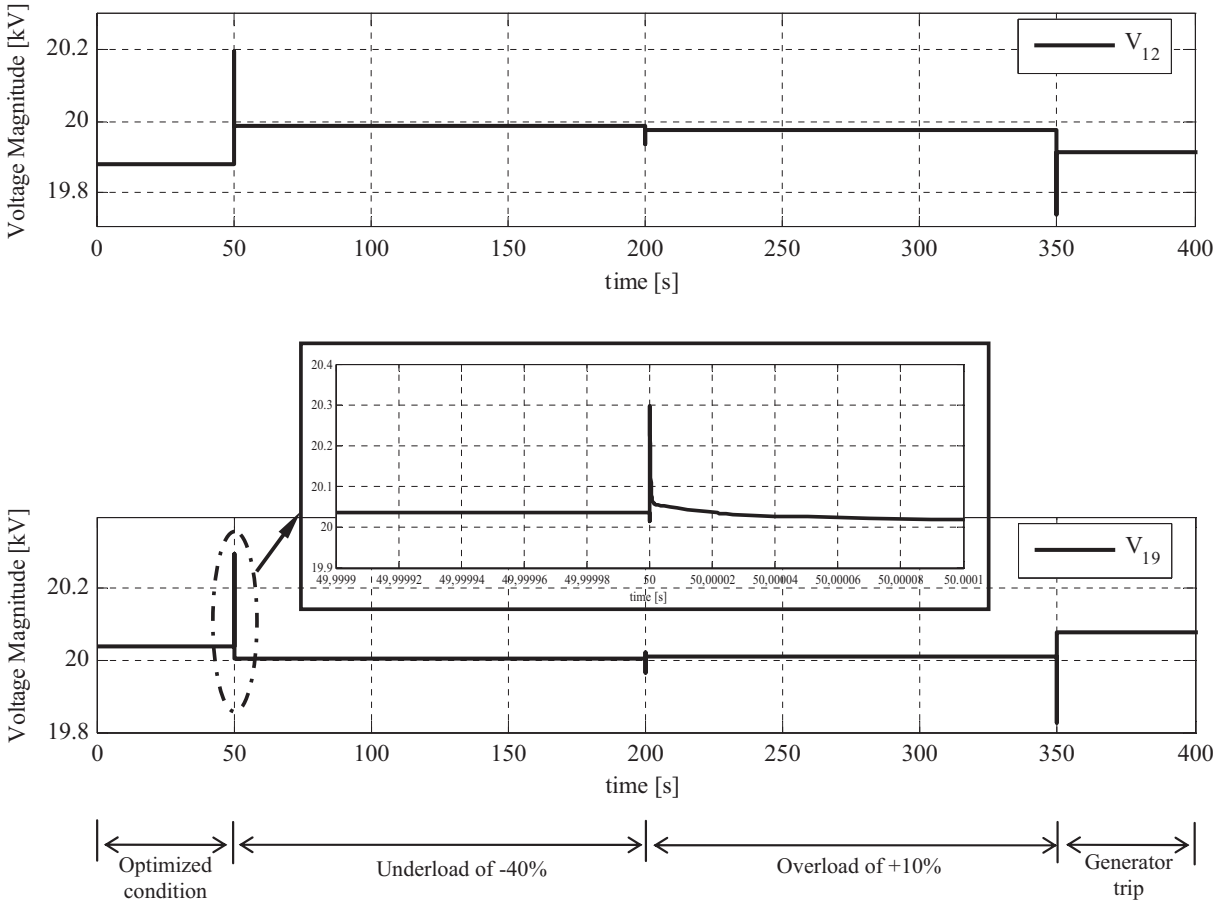
**Fig. 11.** Time domain behavior of the nodal voltages experiencing the greater voltage deviation from the reference value.

settling times less than $10^{-5}$. This settling time is fully compatible with usual sampling times of real scada systems.

Choosing the suggested value of $k$, the reactive power control laws, $\boldsymbol{Q}_{PV}$, were generated as shown in Fig. 7. Note that, reactive power curves refer to the power that must be provided by each of the two inverters of all plants.

As can be seen, the controller rapidly forces each inverter to inject its maximum allowable reactive power, equal to 0.866 MVAr.

Depending on individual contributions to the objective function, each generator reaches its saturation limit at different times.

As shown in Fig. 8, with these control actions the nodal system voltages were forced to be very close to the assumed reference value.

Fig. 9 shows the time domain behavior of the performance index $V$. As can be noted, it monotonically decreases from the value 4.57 $kV^2$ to its minimum value, equal to 0.05 $kV^2$, with an
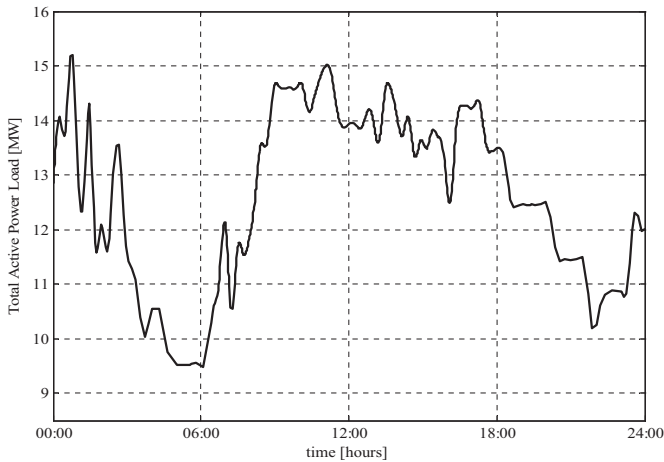


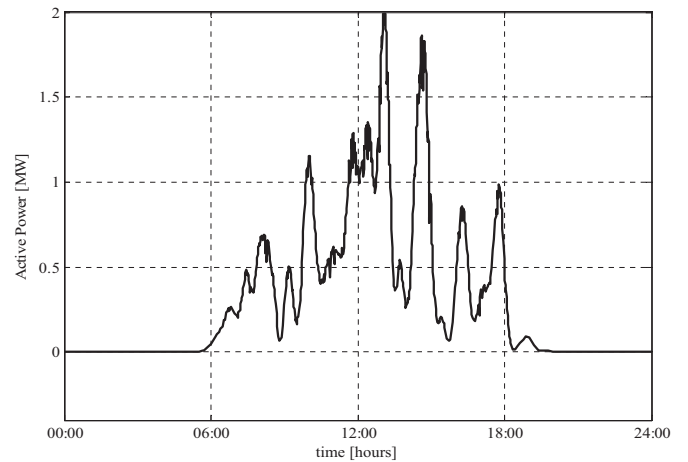**Fig. 12.** Daily load profile of the system under investigation.



**Fig. 13.** Daily generation profile of the two inverters of each PV plant.
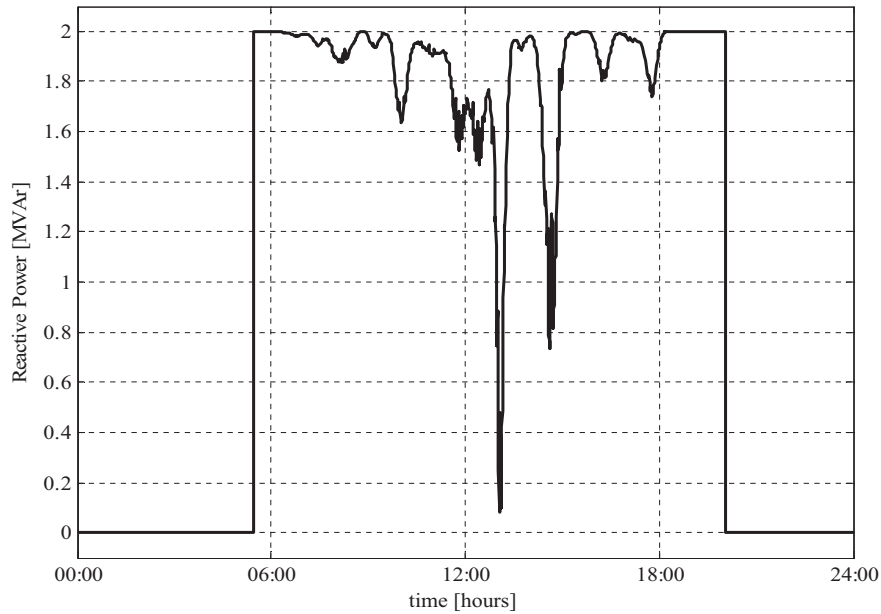
**Fig. 14.** Daily behavior of the reactive power provided by the PV plant at bus # 11.

improvement equal to 98.9%. *V* could not reach the zero (corresponding to an improvement equal to 100%) because the control action is constrained by the generator capability curves.

### 5.2. Test 2 — sequential events — underload, overload and generator trip

The controller's ability to be auto-adaptive was investigated by simulating the following sequential scenarios starting from the previous optimized condition:

- a sudden underload evenly distributed equal to −40% of the base load at *t* = 50 s;

- a sudden overload evenly distributed equal to +10% of the previous load condition at *t* = 200 s;
- a generator trip (at bus #11) occurring at *t* = 350 s.

Fig. 10 shows the time domain behaviors of the obtained control laws.

For clarity purposes, in Fig. 11 we report only the time domain behaviors of the nodal voltages at buses 12 and 19 experiencing the largest voltage deviations. In the time interval [50 s, 200s[, the given underload implies a rapid rise in the nodal voltages, particularly on bus 19. In response to this, the algorithm modulates all reactive injections, trying to optimize the voltage deviations from the reference value. At the post disturbance equilibrium point, PV
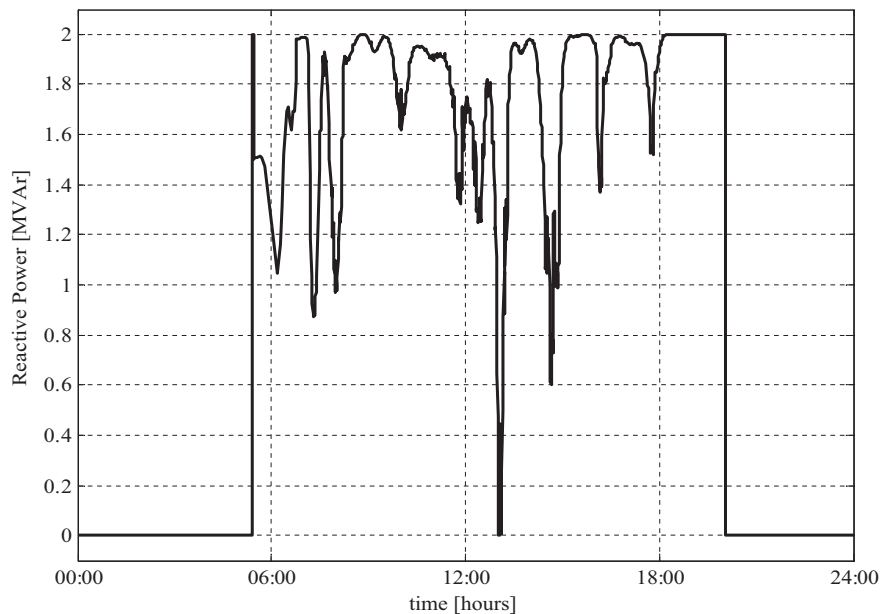


**Fig. 15.** Daily behavior of the reactive power provided by the PV plant at bus # 22.
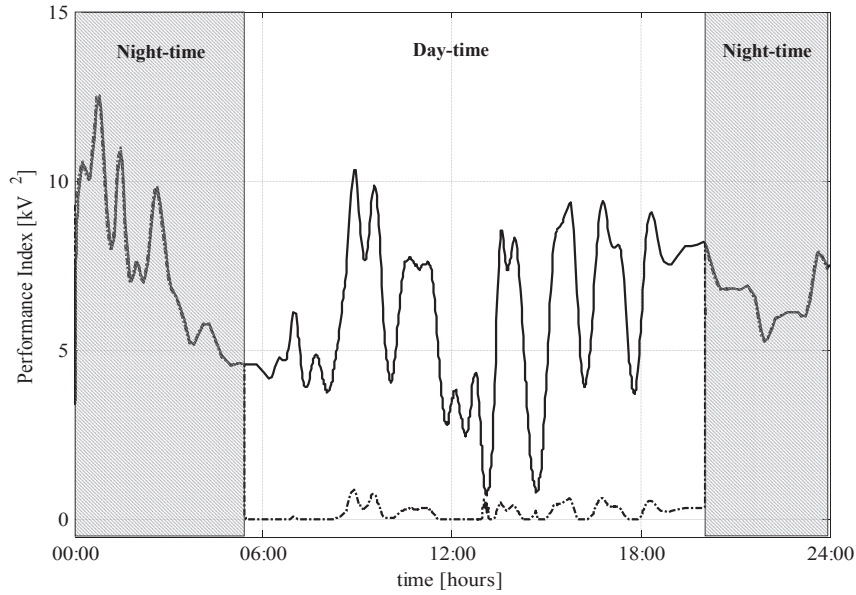
**Fig. 16.** Daily profile of the objective function: with (dotted line) and without (solid line) the control action.

**Table 2**
Performance Index for different values of time delays.[a]

| Delay time | 0 s (Continuous time behavior) | 10 s | 1 min | 5 min | 15 min |
|---|---|---|---|---|---|
| Performance index $V$ [kV$^2$h] | 69.40 | 69.42 | 69.48 | 69.52 | 70.00 |

[a] The performance indexes have been evaluated considering the regulation acting during the daytime over a time window of 24 h.

plants connected at buses 11, 15 and 16 reach their upper limits, whereas the generator at bus 19 reduces its injection to the value of 0.94 MVAr, and the reactive power at bus 22 completely reverses from the value of 1.732 MVAr to the value of −0.51 MVAr (Fig. 10).

The intervention of the limits at buses 11, 15 and 16 precludes the exact achievement of the target 20 kV.

Following the overload occurrence at time $t = 200$ s, the proposed algorithm produced the new optimal condition, only moving the reactive power generated at bus 19.

As a consequence of the generator tripping at time $t = 350$ s, the algorithm reacted by sharing the control burden previously assigned to the tripped generator among the remaining PV plants. In particular, the exigency of reactive power was satisfied only by the generators that had not yet reached their maximum values, i.e. plants 19 and 22.

The given scenarios were characterized by the following steady-state values of the performance index $V$:
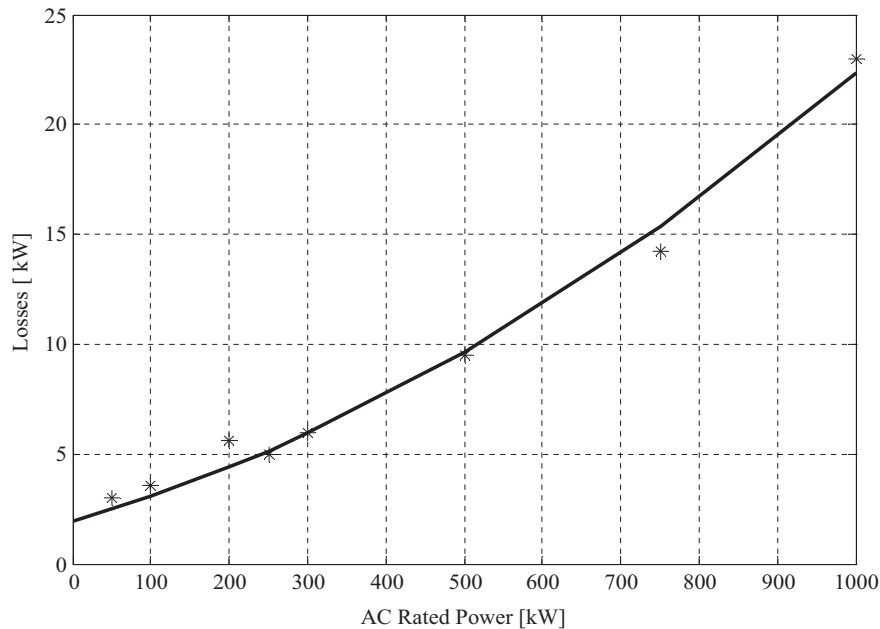
- underload of −40%: $V = 1.9 \cdot 10^{-3}$ kV$^2$;



**Fig. 17.** Available loss data and the fitting power loss curve of the PV inverter Conergy CSI 1000 [37].

| PCC [#] | Daily energy loss without the reactive service [kWh/day] | Daily energy loss with the reactive service [kWh/day] | Daily additional energy losses due to the reactive power provision $E_{loss}^{Q_{pv}}$ [kWh/day] | Daily additional costs [€/day] |
|---------|-----------|-----------|-----------|-----------|
| 11 | 201.34 | 685.78 | 484.42 | 85.74 |
| 15 | 217.92 | 686.60 | 468.70 | 82.94 |
| 16 | 219.54 | 686.74 | 447.54 | 79.22 |
| 19 | 215.16 | 686.42 | 471.28 | 83.42 |
| 22 | 203.92 | 643.98 | 440.06 | 77.88 |
| **Total costs** | | | | **409.2** |

- overload of +10%: $V = 3.4 \cdot 10^{-3}$ kV$^2$;
- generator trip: $V = 27.1 \cdot 10^{-3}$ kV$^2$.

### 5.3. Test 3 — real-time operation

The ability of the proposed controller to operate in real-time was tested by considering daily fluctuations for the load as well as for the generation. We used recorded data for the daily load profile of an existing MV feeder (Fig. 12) and for the active power produced by an existing PV plant (Fig. 13).

We replicated the given generation profile for all generators engaged in our network. Moreover, we differentiated these power outputs by adding a white noise having variance equal to 0.1. In this way, slight differences in solar radiation or environmental factors (ambient and cells operating temperatures, humidity etc.) specifically affecting each PV plant are taken into account, giving rise to a more realistic simulation.

In order to avoid greater costs for the reactive compensation occurring if inverters do not produce active power, we assumed that the controller only acts when the inverter is turned on, i.e. it is activated in the day-time (05:25 am ÷ 08:00 pm).

In Figs. 14 and 15 we report only the obtained control laws for the PV plants "called" to provide the greatest (bus #11) and the least (bus #22) amount of the daily reactive energy. From a comparison with Fig. 13, it can be observed that when the active power reaches it maximum value (at about 01:00 pm), the reactive power vanishes guaranteeing incomes deriving from selling the active energy.

In Fig. 16 we show the comparison of the daily behavior of the performance index with and without the control action.

In order to give a measure of the effectiveness of the proposed methodology, we adopted the following integral index:

$$V_{daily} = \int_{t=00:00}^{t=24:00} V(t) \mathrm{d}t$$

In this case, the controller was able to reduce the performance index from a value of $V_{daily}^{non-opt} = 154.33$ kV$^2$h in the non-optimized condition to a value of $V_{daily}^{opt} = 69.4$ kV$^2$h, giving rise to an improvement equal to 55.0%.

Time delays due to congestion or failures of the communication system could negatively impact the performance of any control system. In order to understand how the developed controller is capable of treating data affected by significant time delays, we supposed that measurements and signals coming from/to the field were delayed by 10 s, 1 min, 5 min and 15 mins. The main results of this analysis are reported in Table 2.

We also analyzed costs due to the reactive support in the considered day. As discussed in Section 3, additional energy losses can be evaluated by means of Eqn. (15) as the difference between the daily energy lost with and without the reactive power control.

The loss curve of the chosen inverter (Fig. 17) was fitted by a second order polynomial curve whose coefficients were $\alpha = 1.7413$ kW; $\beta = 0.0112$ kW/kVA; $\gamma = 0.00001$ kW/kVA$^2$.

In Table 3 we report the daily energy lost with and without the reactive power control, as well as the related additional losses for the considered day.

The daily additional operational costs are reported in the last column. These costs were evaluated by adopting the current Italian feed-in-tariff for PV plants equal to $FIT = 0.099$ €/kWh [39] and the compensation for the energy not supplied equal to $C_{ENS} = 0.0644$ €/kWh [40].

As can be noted, the provision of reactive power implied an additional cost of about 410 €/day, corresponding to about 82 €/day for each plant.

## 6. Conclusions

In this paper, a centralized voltage control scheme has been developed by adopting grid-connected photovoltaic plants as reactive power providers. The proposed controller is based on a self-adaptive optimization procedure which involves a fictitious dynamic system producing control laws to be sent to local controllers of PV-inverters. The proposed controller has been tested on a typical MV distribution network under different operating conditions. The results obtained demonstrate that the suggested control system promptly reacts to suddenly burdensome events such as underload, overload and generators tripping. With this characteristic, the automatic controller can be fruitfully implemented in real-time, as confirmed by simulations performed on a typical day. The controller also complies with the unavailability of one or more PV generators to supply the required amount of reactive power. In fact, in this case, the control burden is automatically shared among the remaining PV plants, giving rise to a suboptimal condition. The algorithm can also provide the evaluation of additional costs incurred for the provision of this ancillary service as additional information for the grid operator as well as the PV owners. This element can be fruitfully adopted in order to build a fair compensation mechanism, thus stimulating the provision of this important ancillary service.

## Appendix A. Data for the test system

| Bus [#] | Active power [MW] | Reactive power [MVAr] | Bus [#] | Active power [MW] | Reactive power [MVAr] |
|---------|-----------|-----------|---------|-----------|-----------|
| 1 | Slack bus | Slack bus | 12 | 1.01 | 0.29 |
| 2 | 1.01 | 0.29 | 13 | 1.01 | 0.29 |
| 3 | 0.80 | 0.23 | 14 | 1.01 | 0.29 |
| 4 | 1.01 | 0.29 | 15 | 0.50 | 0.15 |
| 5 | 0.80 | 0.23 | 16 | 1.01 | 0.29 |
| 6 | 0.30 | 0.09 | 17 | 0.00 | 0.00 |
| 7 | 0.00 | 0.00 | 18 | 1.01 | 0.29 |
| 8 | 1.01 | 0.29 | 19 | 1.01 | 0.29 |
| 9 | 0.00 | 0.00 | 20 | 0.00 | 0.00 |
| 10 | 1.01 | 0.29 | 21 | 0.50 | 0.15 |
| 11 | 1.01 | 0.29 | 22 | 0.30 | 0.09 |

**Table A2**

—Line data.

| Line [#] | From [#] | To [#] | R [Ω] | X [Ω] |
|---|---|---|---|---|
| 1 | 1 | 2 | 0.144 | 0.196 |
| 2 | 2 | 3 | 0.108 | 0.147 |
| 3 | 3 | 4 | 0.163 | 0.179 |
| 4 | 4 | 5 | 0.205 | 0.225 |
| 5 | 5 | 6 | 0.172 | 0.188 |
| 6 | 6 | 7 | 0.174 | 0.191 |
| 7 | 7 | 8 | 0.149 | 0.164 |
| 8 | 8 | 9 | 0.165 | 0.181 |
| 9 | 9 | 10 | 0.249 | 0.122 |
| 10 | 10 | 11 | 0.283 | 0.139 |
| 11 | 11 | 12 | 0.249 | 0.122 |
| 12 | 12 | 13 | 0.277 | 0.136 |
| 13 | 13 | 14 | 0.218 | 0.107 |
| 14 | 14 | 15 | 0.302 | 0.148 |
| 15 | 9 | 16 | 0.115 | 0.096 |
| 16 | 16 | 17 | 0.109 | 0.092 |
| 17 | 17 | 18 | 0.202 | 0.099 |
| 18 | 18 | 19 | 0.474 | 0.232 |
| 19 | 17 | 20 | 0.297 | 0.146 |
| 20 | 20 | 21 | 0.381 | 0.187 |
| 21 | 21 | 22 | 0.318 | 0.156 |

## References

[1] Italian legislative Decree 109, DM 5/5/2011, "Quarto Conto Energia per il fotovoltaico-Incentivazione della produzione di energia elettrica da impianti solari fotovoltaici".

[2] Gross A, Bogensperger J, Thyr D. Impact of large-scale photovoltaic systems on the low voltage network. Sol Energy 1997;59(4–6):143–9.

[3] Thornycroft JM, Jenkins N, Strbac G, Bates JR. PV power supply interaction with the supply network: system analysis. In: 1998 World conference and exhibition on photovoltaic solar energy conversion, Vienna, Austria; 1998.

[4] Begović M, Pregelj A, Rohatgi A, Novosel D, "Impact of renewable distributed generation on power systems", 34th annual Hawaii international conference on system sciences (HICSS-34)-Volume 2, Maui, Hawaii January 03–January 06.

[5] Hernández JC, Medina A, Jurado F. Impact comparison of PV system integration into rural and urban feeders. Energy Convers Manag 2008;49:1747–65.

[6] González C, Villafáfila R, Ramírez R, Sudrià A, Sumper A. Assess the impact of photovoltaic generation systems on low-voltage network: software analysis tool development. In: Proceedings of the 9th international conference on electrical power quality and utilisation, 9–11 October, Barcelona; 2007.

[7] Italian Electrotechnical Committee (CEI). Technical standard CEI 11-20 "Electrical energy production system and uninterruptable power systems connected to I and II class network [in Italian]. 4th ed. Milan: CEI; 2000.

[8] "IEEE 1547 Standard for interconnecting distributed resources with electric power systems." [Online]. Available: http://grouper.ieee.org/groups/scc21/1547/1547 index.html.

[9] Transmission Code. 2007-Network and system rules of the german transmission system operators, Verband der Netzbetreiber VDN eV. Berlin: Beim VDEW; August, 2007.

[10] Technical Guideline. Generating plants connected to the medium-voltage network – guideline for generating plants' connection to and parallel operation with the medium voltage network. Berlino: BDEW; June 2008.

[11] CEI 0–16. Regola tecnica di riferimento per la connessione di Utenti attivi e passivi alle reti AT ed MT delle imprese distributrici di energia elettrica. 2nd ed. July, 2008. 9404.

[12] Ellis A. Interconnection standards for PV systems. Cedar Rapids IA; October, 2009.

[13] Progetto di norma CEI C 1058. Regola tecnica di riferimento per la connessione di utenti attivi e passivi alle reti BT delle imprese distributrici di energia elettrica. June, 2010.

[14] Tuohy A. Grid code evolution in Europe. In: Atti della 4th international conference on the integration of renewable and distributed energy resources, Albuquerque; December, 2010.

[15] Frank C.J. Lin. and Oliver S. Yu, "Transmission system planning for renewable energy developments in Taiwan", Proceedings of AESIEAP 18th conference of the electric power supply industry Taipei, Taiwan, 24–28 October, 2010.

[16] Troester E, "New German grid codes for connecting PV systems to the medium voltage power grid", Proceedings of the 2nd international workshop on concentrating photovoltaic power plants: optical design, production, grid connection.

[17] Allegato A 70. Regolazione tecnica dei requisiti di sistema della generazione distribuita. Codice di Terna. 2012.

[18] EN 50160. Voltage characteristics of electricity supplied by public distribution systems. 1999.

[19] Lopes JAP, Mendonça Â, Fonseca N, Seca L. Voltage and reactive power control provided by DG units. In: CIGRE symposium: power systems with dispersed generation; April 2005. Athens, Greece.

[20] Delfino F, Denegri GB, Invernizzi M, Procopio R. An integrated active and reactive power control scheme for grid-connected photovoltaic production systems. In: Proceedings of the IEEE 39th power electronics specialists conference PESC; 2008. 15–19 June, Rhodes, 2008.

[21] Angelino R, Bracale A, Carpinelli G, Lauria D, Mangoni M, Proto D, "Centralized control of dispersed generators providing ancillary services in distribution networks part i: theoretical aspects", IEEE/PES international conference UPEC 2009, September 1–4, 2009, Glasgow (GB).

[22] Malekpour AR and Pahwa A, "Reactive power and voltage control in distribution systems with photovoltaic generation", Proceeding of the North American power symposium (NAPS) 2012, September 9–11, 2012.

[23] O. Richardot, A. Viciu, Y. Bésanger, N. Hadjsaïd and C. Kieny "Coordinated Voltage Control in Distribution Networks Using Distributed Generation", Transmission and Distribution Conference and Exhibition, 2005/2006 IEEE PES, 21–24 May 2006, 1196 − 1201.

[24] Vovos PN, Kiprakis AE, Wallace AR, Harrison GP. Centralized and distributed voltage Control: impact on distributed generation penetration. IEEE Transaction Power Syst 2007;22(1):476–83.

[25] Toma S, Senjyu T, Yona A, Sekine H, Funabashi T and Kim C, "Optimal control of voltage in distribution systems by voltage reference management", Proceedings of 2nd IEEE international conference on power and energy (PECon 08), December 1–3, 2008, Johor Baharu, Malaysia.

[26] Madureira AG, Peças Lopes JA. Coordinated voltage support in distribution networks with distributed generation and microgrids. IET Renew Power Gener 2009;3(4):439–54.

[27] Kusiak A, Wei XP. Optimization of the activated sludge process. ASCE J Energy Eng 2013;139(No. 1):12–7.

[28] Debnath S, n. Rup, Ray. THD optimization in 13 level photovoltaic inverter using genetic algorithm. Int J Eng Res Appl 2013;2(3):385–9.

[29] Cagnano A, Torelli F, Alfonzetti F, De Tuglie E. Can PV plants provide a reactive power ancillary service? A treat offered by an on-line controller. Renew Energy 2011;36(3):1047–52.

[30] Cagnano A, De Tuglie E, Liserre M, Mastromauro RA. Online optimal reactive power control strategy of PV inverters. Ind Electron IEEE Trans 2011;58(10):4549–58.

[31] M. Braun, "Reactive power supplied by PV inverters − cost-benefit analysis", In: 22nd European photovoltaic solar energy conference and exhibition, Milan, Italy; 3–7 September 2007.

[32] Braun M, "Reactive power supply by distributed generators", IEEE-power and energy society general meeting − conversion and delivery of eletrical energy in the 21st century, Pittsburgh, USA, 20–24 July, 2008.

[33] Braun M, Stetz T, Reimann B, Valov B, Arnold G. Optimal reactive power supply in distribution networks-technological and economic assessment. In: 24th European photovoltaic solar energy conference and exhibition, Hamburg; 2009.

[34] Haghighat H, Kennedy S, "A model for reactive power pricing and dispatch of distributed generation", IEEE-power and energy society general meeting, pp. 1–10, Minneapolis, 25–29 July, 2010.

[35] Stott B. Review of load-flow calculation methods. IEEE July, 1974;62(7):916–29.

[36] Suda N. PID control. (System, Control and Information Library, NO.6). Asakura; 1992 (in Japanese).

[37] Conergy CIS 400–1200. [online] Available: http://www.conergy.it/PortalData/15/Resources/products/photovoltaics/inverters/pdf/TD_Conergy_CIS_400-1400_(ENhttp://www.conergy.it/PortalData/15/Resources/products/photovoltaics/inverters/pdf/TD_Conergy_CIS_400-1400_(EN).pdf.

[38] Matlab/Simulink user's guide, The Math Works.

[39] Italian Legislative Decree 109, DM 5/7/2012, "Quinto Conto Energia − Incentivi per energia da fonte".

[40] GME, "Relazione annual 2010". [online] Available: http://www.mercatoelettrico.org/it/MenuBiblioteca/documenti/20120711RelazioneAnnuale2011.pdf.